

# REDSHIFT-SPACE DISTORTIONS OF GROUP AND GALAXY CORRELATIONS IN THE UPDATED ZWICKY CATALOG

NELSON D. PADILLA, MANUEL E. MERCHÁN, CARLOS A. VALOTTO AND DIEGO  
G. LAMBAS

nelsonp, manuel, val, dgl @oac.uncor.edu

Grupo de Investigación en Astronomía Teórica y Experimental (IATE), Observatorio  
Astronómico, Laprida 854, Córdoba and CONICET, Argentina.

AND

MARCIO A. G. MAIA

maia@on.br

Departamento de Astromomia, Observatório Nacional, Rua General José Cristino 77, Rio de  
Janeiro, 20921-400, Brazil.

*Draft version March 19, 2022*

## ABSTRACT

The two-point correlation function is computed for galaxies and groups of galaxies selected using 3-dimensional information from the Updated Zwicky Galaxy Catalog - (UZC). The redshift space distortion of the correlation function  $\xi(\sigma, \pi)$  in the directions parallel and perpendicular to the line of sight, induced by pairwise group peculiar velocities is evaluated.

Two methods are used to characterize the pairwise velocity field of groups and galaxies. The first method consists in fitting the observed  $\xi(\sigma, \pi)$  with a distorted model of an exponential 1-dimensional pairwise velocity distribution, in fixed  $\sigma$  bins. The second method compares the contours of constant predicted correlation function of this model with the data. The results are consistent with a 1-dimensional pairwise rms velocity dispersion of groups  $\langle w^2 \rangle^{1/2} = 250 \pm 110 \text{ km s}^{-1}$ . We find that UZC galaxy 1-dimensional pairwise rms velocity dispersion is  $\langle w^2 \rangle^{1/2} = 460 \pm 35 \text{ km s}^{-1}$ . Such findings point towards a smoothly varying peculiar velocity field from galaxies to systems of galaxies, as expected in a hierarchical scenario of structure formation.

We find that the real-space correlation functions of galaxies and groups in UZC can be well approximated by power laws of the form  $\xi(r) = (r/r_0)^\gamma$ . The values of  $\gamma$  for each case are derived from the correlation function in projected separations  $\omega(\sigma)$ . Using these estimates we obtain  $r_0$  from the projected correlation functions. The best fitting parameters are  $\gamma = -1.89 \pm 0.17$  and  $r_0 = 9.7 \pm 4.5 \text{ } h^{-1} \text{ Mpc}$  for groups, and  $\gamma = -2.00 \pm 0.03$  and  $r_0 = 5.29 \pm 0.21 \text{ } h^{-1} \text{ Mpc}$  for galaxies.

The  $\beta$ -parameter ( $\beta = \Omega^{0.6}/b$ ) is estimated for groups and galaxies using the linear approximation regime relating real and redshift-space correlation functions. We find  $\beta_{gx} = 0.51 \pm 0.15$  for galaxies, in agreement with previous works, while for groups we obtain a noisy estimate  $\beta < 1.5$ .

Both methods used to characterize the pairwise velocity field are also tested on mock catalogs taken from CDM numerical simulations. The results show that the conclusions derived from the application of both methods to the observations are reliable. We also find that the second method, developed in this paper, provides more stable and precise results.

## 1. INTRODUCTION

The lack of homogeneity of the matter distribution on small scales, produces local departures of the Hubble flow, inducing streaming motions

of galaxies into the direction of larger concentrations of matter like clusters of galaxies or filaments. The determination of the amplitude of peculiar velocities is important, since it is dependent on the cosmological matter density parameter,  $\Omega$ . Thus, there is a possibility to constrain the value of  $\Omega$  using the non-Hubble component of galaxy motions. A characterization of this peculiar velocity field can be obtained by measuring the apparent distortion of the clustering pattern in the two-point correlation function for galaxies in redshift space,  $\xi(\sigma, \pi)$ , where  $\sigma$  and  $\pi$  are the separations perpendicular and parallel to the line of sight, respectively. The anisotropy of the correlation function in redshift space depends on the peculiar velocity distribution function. On non-linear scales virialized regions dominate, inducing the well known “Finger of God” effect, seen in redshift surveys allowing for estimates of the galaxy one-dimensional pairwise rms velocity dispersion  $\langle w^2 \rangle^{1/2}$  (Davis & Peebles 1983). On larger scales, where the linear regime applies, velocities are dominated by the infall into overdense regions as bulk motion of galaxies are generated by new levels of clustering. This effect results in a compression of the  $\xi$  contours along the line of sight direction ( $\pi$ ), and allows estimates of the parameter  $\beta = \Omega^{0.6}/b$  (Kaiser (1986)), where  $b$  is the linear bias parameter. Extensive studies of  $\xi(\sigma, \pi)$  for galaxies have been carried out (see for instance, Loveday et al. (1996), Ratcliffe et al. (1998b), Tadros et al. (1999), and references therein). The results of the different galaxy surveys are consistent with a one-dimensional pairwise velocity dispersion  $\langle w^2 \rangle^{1/2} \simeq 400 \pm 50 \text{ km s}^{-1}$ , and parameter  $\beta_{gx} \simeq 0.5 \pm 0.15$ .

To examine larger volumes, clusters and groups of galaxies can be used as suitable tracers of the large scale structure of the universe. Several works have characterized the clustering properties of rich clusters of galaxies (see for instance Croft et al. (1997) and Abadi, Lambas & Muriel (1998)) concluding that the cluster autocorrelation function has a similar shape to that of galaxies, only with a larger amplitude. An analogous conclusion was also obtained for groups of galaxies (e.g., Merchán, Lambas & Maia (2000)). Due to the fact that the amplitude of the correlation function of galaxy systems is significantly larger than that corresponding to galaxies, it is expected a more significant contribution by the mean streaming velocity term. By contrast, galaxies with sim-

ilar peculiar velocities would appear strongly distorted along the line of sight due to their smaller correlation amplitude. Small scales effects, such as galaxy velocity bias and strongly non-linear regimes would not be present in the analysis of groups which could provide a more suitable estimate of the mean relative motions at intermediate and large scales.

The subject of this paper is about redshift space distortions of galaxies and groups of galaxies. We study a sample of galaxies obtained from the Updated Zwicky Catalog (UZC, Falco et al. (1999)) and groups of galaxies (GUZC) obtained from this catalog using a friends-of-friends algorithm (Merchán, Lambas & Maia (2000)). The properties of these samples are briefly described in section 2. In section 3, we estimate the pairwise characteristic velocity for groups applying a minimum  $\chi^2$  analysis to the parameters of the exponential velocity distribution model. We also estimate the  $\beta$  parameter. For comparison, we repeat the calculations for the galaxy parent catalog and compare our results with estimates from other works. In section 4, we test the adequacy of the methods applied to estimate  $\langle w^2 \rangle^{1/2}$  and  $\beta$  using mock catalogs taken from numerical simulations corresponding to the empirical power spectrum (Peacock 1997) which reproduces the global properties of galaxy clustering. Conclusions are summarized in section 5.

## 2. DATA

The sample of galaxies was drawn from the UZC, containing 19,369 objects with apparent Zwicky magnitudes  $m_{Zw} \leq 15.5$  and with 96% completeness in redshift. The region covered by the catalogue is  $20^h \leq \alpha_{1950} \leq 4^h$  and  $8^h \leq \alpha_{1950} \leq 17^h$  and  $-2.5^\circ \leq \delta_{1950} \leq 50^\circ$ , providing accurate coordinates within 2" and reliable redshifts in the range  $cz = 0 - 25,000 \text{ km s}^{-1}$  with a reasonably complete sky coverage (see Falco et al. (1999) for more details). For our statistical purposes, we have considered galaxies with galactic latitudes  $|b| > 20^\circ$  to avoid galactic obscuration. Moreover, given the strong density gradient beyond  $cz = 15,000 \text{ km s}^{-1}$  we adopted this limit in  $cz$ .

The algorithm adopted by Merchán, Lambas & Maia (2000) for the construction of the catalog of groups of galaxies is basically the one described by Huchra & Geller (1982) with the improvements by Maia, da Costa & Latham (1989) and by Ramella

Pisani & Geller (1997) in order to minimize the number of interlopers. The groups present a surrounding density contrast ( $\delta\rho/\rho$ ), relative to the mean density of galaxies of 80. The UZC group catalog (GUZC) contains systems with at least 4 members and mean radial velocities,  $V_{gr} \leq 15,000 \text{ km s}^{-1}$  consistent with the galaxy catalog. From the GUZC catalog we have considered groups with the same restrictions in galactic latitude and declination than those of the galaxy catalog ( $|b| = 20^\circ$  and  $-2.5^\circ < \delta < 50^\circ$ ). Very rich groups containing more than 40 galaxies were not considered (only 6 groups) in the sample to avoid few nearby large clusters and structures possibly related to systematics in the identification procedure biasing towards large percolating structures. In addition to the above criteria, those groups with  $V_{gr} \leq 2,000 \text{ km s}^{-1}$  were also discarded, to prevent any significant contribution of the group peculiar velocities in the measured redshifts which were used to determine their distances. With all the restrictions applied, the final sample is made up of 513 groups.

### 3. ANALYSIS

We analyze the effects of the peculiar velocity field on the correlation function of groups and galaxies as a function of the separations  $\sigma$  and  $\pi$ . To compute  $\xi(\sigma, \pi)$  we generate a random catalog with the same angular limits and radial selection function than the sample of objects. We cross correlate data-data and random-random pairs ( $N_{dd}$  and  $N_{rr}$  respectively) binning them as a function of separation in the two variables  $\sigma$  and  $\pi$ . Our estimate of  $\xi(\sigma, \pi)$  is (Davis & Peebles 1983):

$$\xi(\sigma, \pi) = \frac{N_{dd}n_R^2}{N_{rr}n_D^2} - 1 \quad (1)$$

where  $n_D$  and  $n_R$  are the number of data and random points respectively.

This estimator is sensitive to uncertainties in the mean density compared to more stable estimators (eg. Hamilton 1993). However, since our analysis is confined to the most inner scales where the correlation function has a large amplitude, there is not a real need to use these alternatives.

The random catalog has 400 times more objects than the data sample to minimize fluctuations. To calculate  $\xi(\sigma, \pi)$  for galaxies we have adopted the same cuts in radial velocity and galactic latitude than for the sample of groups to make the results more comparable. Within these restrictions,

the final sample of galaxies comprises 14,755 objects.

In Figure 1 are displayed the levels of equal amplitude of the 2-point correlation function of groups (panel a) and galaxies (panel b) in the coordinates  $\sigma$  and  $\pi$ . It can be appreciated the compression of the groups iso-correlation curves in the  $\pi$  direction which indicates the lack of high pairwise velocities in the sample of these systems of galaxies. From the comparison with clusters derived from surveys in two dimensions it is clear the existence of either large pairwise velocities or large projection biases as discussed by Sutherland (1988). The presence of such projection biases in cluster samples derived in two dimensions has also been pointed out by van Haarlem, Frenk & White (1997) and by Valotto, Moore & Lambas (2000). The sample of groups analyzed in this paper is derived from a nearly complete spectroscopic survey, so that we would not expect the artificial strong elongation along the line of sight observed in samples of clusters identified in two dimensions. This elongation would be originated by the systematic presence of groups along the line of sight in the fields of 2-dim clusters. From the theoretical point of view, such strong elongations along the line of sight are not expected in a hierarchical scenario of structure formation. This is confirmed by the compression observed in panel (a) and provides a clear evidence for the infall of groups onto larger structures. The level contours are well defined in the non-linear and mildly-linear regime  $\xi(\sigma, \pi) \lesssim 1$ . The analysis developed in the next sections will therefore consider these level contours. Due to the larger velocities of galaxies and their smaller correlation amplitude, it can be seen in panel (b) of this figure a large distortion of the iso-correlation curves in the  $\pi$  direction. This is a direct consequence of the large relative peculiar velocities associated to the non-linear regime at small galaxy separations.

#### 3.1. Estimates of $\langle w^2 \rangle$

In order to characterize the pairwise velocities of galaxies and groups in UZC from the correlation redshift-space distortion map, we have used two different procedures. The first method corresponds to that adopted by Loveday et al. (1996) and Ratcliffe et al. (1998b). We compare the observed correlation function  $\xi(\sigma, \pi)$  with the convolution of the real-space correlation function with

the pairwise velocity distribution function  $f(w)$  (Bean et al. 1983 )

$$1 + \xi(\sigma, \pi) = \int_{-\infty}^{\infty} [1 + \xi(r)] f[w' + H_0 \beta \xi(r) (1 + \xi(r))^{-1} r'] dw' \quad (2)$$

where  $r^2 = r'^2 + \sigma^2$ , and  $H_0$  is the Hubble constant,  $r' = \pi - w'/H_0$  (the prime denotes the line-of-sight component of a vector quantity) and  $\langle w \rangle \simeq -H_0 \beta \xi(r) (1 + \xi(r))^{-1} r'$  is the mean streaming velocity of galaxies at separation  $r$ . We have calculated the best-fit rms peculiar velocity  $\langle w^2 \rangle^{1/2}$  for an exponential distribution,

$$f(w) = \frac{1}{\sqrt{2} \langle w^2 \rangle^{1/2}} \exp \left( -\sqrt{2} \frac{|w|}{\langle w^2 \rangle^{1/2}} \right) \quad (3)$$

We adopted this pairwise velocity distribution because it has proved to be the most accurate fit to the results from numerical simulations as it has been shown by Ratcliffe et al. (1998b).

We use a power-law model for  $\xi(r)$  with an index  $\gamma$  derived from the correlation function in projected separation  $\omega(\sigma)$ ,  $\gamma = \gamma_p - 1$ , where  $\gamma_p$  corresponds to the power law fit of the projected two-point correlation function. The projected correlations for groups and galaxies and the corresponding power-law fits ( $\gamma_p = -0.89 \pm 0.17$  and  $\gamma_p = -1.00 \pm 0.03$  for groups and galaxies respectively), are shown in Figure 2.

The optimum value of  $\langle w^2 \rangle^{1/2}$  for this distribution was calculated for fixed  $\sigma$  bins by minimizing the quantity  $\chi^2$ ,

$$\chi^2 = \sum_{\pi bins} [\xi^o(\sigma, \pi) - \xi^p(\sigma, \pi)]^2 \quad (4)$$

where  $\xi^o(\sigma, \pi)$  is the observed redshift space correlation function, and  $\xi^p(\sigma, \pi)$  is the predicted correlation function from equation 2. The values of  $\chi^2$  were calculated for different  $r_0$  and  $\langle w^2 \rangle^{1/2}$ , and its minimum indicates the best pair of values  $r_0$  and  $\langle w^2 \rangle^{1/2}$ . The errors were obtained repeating the previous  $\chi^2$  procedure for 50 bootstrap resamplings. The resulting values of  $\langle w^2 \rangle^{1/2}$  for groups and galaxies are shown in tables 1 and 2. The minimum  $\chi^2$  values are  $\langle w^2 \rangle^{1/2} = 390 \pm 185 \text{ km s}^{-1}$  and  $\langle w^2 \rangle^{1/2} = 520 \pm 95 \text{ km s}^{-1}$  for groups and galaxies respectively.

The second method adopted to characterize the pairwise velocity field compares the predicted and

observed contours of constant correlation function. We consider 5 levels of constant correlation:  $\xi(\sigma, \pi) = 0.6, 0.8, 1.0, 1.2$  and  $1.4$ . We describe the equal-correlation contours in polar coordinates  $r$  and  $\theta$  and we find the best fitting values of  $r_0$  and  $\langle w^2 \rangle^{1/2}$  that minimize the quantity  $\chi^2$  by summation over the  $\theta$  bins

$$\chi^2 = \sum_{\theta bins} [r^o(level, \theta) - r^p(level, \theta)]^2 \quad (5)$$

where indexes  $o$  and  $p$  refer to the observed and predicted radial coordinates of the correlation function contour levels, respectively.

The standard deviation is again obtained from the dispersion of the distribution of best  $r_0$ - $\langle w^2 \rangle^{1/2}$  pairs for 50 bootstrap resamplings of the groups. The results for groups and galaxies are shown in table 3. As it can be seen by inspection to this table, this second method gives more stable determinations of  $\langle w^2 \rangle^{1/2}$  (minimum  $\chi^2$  values  $\langle w^2 \rangle^{1/2} = 250 \pm 110 \text{ km s}^{-1}$  and  $\langle w^2 \rangle^{1/2} = 460 \pm 35 \text{ km s}^{-1}$  for groups and galaxies respectively). We note that the resulting value of  $\langle w^2 \rangle^{1/2}$  for galaxies, is a factor 1.8 higher than that of groups due to the high relative velocities of close pairs of galaxies.

Dale et al. (1999) estimate the 1-dimensional peculiar velocity dispersion for a sample of nearby Abell clusters  $\sigma_v = 341 \pm 93 \text{ km s}^{-1}$ . This value can be compared with our estimates of  $\langle w^2 \rangle^{1/2}$  that imply  $\sigma_v^{gr} \lesssim 230 \text{ km s}^{-1}$ , considering the limiting case  $\langle w^2 \rangle = 2\sigma_v^2$  for statistically independent pairwise peculiar velocities.

We notice that neither method 1 nor method 2 provide a suitable constrain to the real space correlation length  $r_0$ . In the next subsection we will estimate  $r_0$  considering the projected correlation function, and use these values to infer the  $\beta$  parameter using the linear theory approximation.

### 3.2. Determination of the $\beta$ -parameter

In the linear regime, the direction-averaged redshift space correlation function,  $\xi(s)$ , and the real space correlation function,  $\xi(r)$ , are related by (Kaiser (1986))

$$\xi(s) \simeq \left( 1 + \frac{2}{3}\beta + \frac{1}{5}\beta^2 \right) \xi(r) \quad (6)$$

We computed the redshift-space correlation functions for galaxies and groups, which are shown in Figure 3 for groups represented by a

solid line and galaxies (dashed line). It can be seen from the inspection of this figure that both correlation functions can be well approximated by a power-law fit over a large range of separations.

We define the projected 2-point correlation function,  $W(\sigma)$ , by

$$W(\sigma) = \int_{-\infty}^{\infty} \xi(\sigma, \pi) d\pi = 2 \int_0^{\infty} \xi(\sigma, \pi) d\pi \quad (7)$$

The real-space correlation function  $\xi(r)$  of groups and galaxies show larger negative slope values than  $\xi(s)$ . For groups we obtain  $\gamma_r \simeq -1.9$  and  $\gamma_s \simeq -1.75$ ; and for galaxies  $\gamma_r = -2.0$ ,  $\gamma_s = -1.6$ . The difference between the two slopes is larger for galaxies than for groups due to their higher pairwise velocity dispersion.

To derive  $r_0$  we use the definition of the Beta function in equation 7, which gives

$$W(\sigma) = \sigma^{1-\gamma} r_0^\gamma \left[ \frac{\Gamma(\frac{1}{2})\Gamma(\frac{\gamma-1}{2})}{\Gamma(\frac{\gamma}{2})} \right] \quad (8)$$

where  $\Gamma(x)$  is the Gamma function and  $\gamma < -1$  is assumed (Ratcliffe et al. (1998a)). We therefore find  $r_0$  for different  $\sigma$  bins, and using equation 6 we obtain the values of  $\beta$ . In order to estimate the rms uncertainty in  $\beta$ , we estimate this parameter for 50 bootstrap resamplings to compute the dispersion around the mean. The results are shown in Figures 4 and 5. We have estimated the real-space correlation length  $r_0$  using the projected correlation function  $W(\sigma)$  in equation 8. Errors are derived from bootstrap resamplings at different values of  $\sigma$ . It can be seen in Figure 4, the large scatter around the mean values for groups (panel a) and galaxies (panel b). From a minimum  $\chi^2$  analysis of the data points shown in both panels of Figure 4, we conclude that  $r_0 = 9.7 \pm 4.5 h^{-1}$  Mpc and  $r_0 = 5.29 \pm 0.21 h^{-1}$  Mpc for  $\sigma \in [1, 12] h^{-1}$  Mpc, are suitable estimates of the correlation length of groups and galaxies respectively.

The relative bias between optical galaxies and UZC groups can be derived from the real-space 2-point correlation functions. Considering  $r_0^{gx} = 5.1 h^{-1}$  Mpc,  $\gamma^{gx} = -1.6$  (Ratcliffe et al. (1998a), this work), and our estimates for groups,  $r_0^{gr} = 8.6 h^{-1}$  Mpc,  $\gamma^{gr} = -1.6$ , we obtain  $b^{gx}/b^{gr} \simeq 1.6$ .

In Figure 5 we show the resulting  $\beta$  parameter computed using equation 6 for UZC groups (panel a), and for galaxies (panel b). The uncertainties

in  $\beta$  are obtained from propagation of errors by means of the standard deviation in  $r_0$ . We estimate a mean value of the  $\beta$  using a minimum  $\chi^2$  statistics across the different  $\sigma$  bins adopting  $\Delta\chi^2 = 1$ . With a very large scatter, our results for  $\beta_{gr} < 1.5$  do not provide a useful constraint. The best  $\beta$  value for galaxies ( $\beta_{gx} = 0.51 \pm 0.15$ ) is consistent with recent estimates from different surveys (Ratcliffe et al. (1998b), Tadros et al. (1999)).

#### 4. TESTS WITH UZC MOCK CATALOGS

To test the reliability of the results obtained in the previous sections we have applied our statistical methods to mock catalogs extracted from N-body simulations. The adopted model corresponds to the empirical power spectrum derived by Peacock (1997) from the observed clustering of galaxies corresponding to a flat universe with matter density parameter  $\Omega = 0.3$ , cosmological constant density  $\Omega_\Lambda = 0.7$  and a Hubble constant of  $H_0 = 65$  km/s Mpc $^{-1}$ . We use  $128^3$  particles in a simulated box of  $200 h^{-1}$  Mpc on a side normalized to  $\sigma_8 = 0.76$ . The mass per particle is  $4.86 \times 10^{11} M_\odot$  so that in the following we will associate one galaxy to each particle. From this box we extract a mock catalog of 51540 particles with the same radial selection function than UZC and 2.5 times the area of the sky covered by UZC. We have also identified 1039 groups in the mock catalog with masses in the same range of virial masses than in the observations using an equivalent procedure to that adopted by Merchán, Lambas & Maia (2000). The values of the one dimensional pairwise velocity dispersion is  $\langle w^2 \rangle^{1/2} = 400$  km s $^{-1}$  for the mock groups and  $\langle w^2 \rangle^{1/2} = 520$  km s $^{-1}$  for particles. The correlation function of particles and groups are well fitted by power laws with  $r_0 = 5.10 \pm 0.28 h^{-1}$  Mpc,  $\gamma = -1.50 \pm 0.08$  for particles and  $r_0 = 8.46 \pm 0.47 h^{-1}$  Mpc,  $\gamma = -1.54 \pm 0.11$  for groups. We show in Figure 6 the two-point correlation function of groups (panel a) and particles (panel b) in the space coordinates  $\sigma, \pi$ . By inspection to this figure it can be appreciated the compression of the groups iso-correlation curves in the  $\pi$  direction similar to that shown in Figure 1. On the other hand, the two-point correlation function of particles in  $\sigma, \pi$  coordinates is strongly distorted along the  $\pi$  direction due to the large pairwise particle velocities as well as their smaller correlation amplitude. These distortions are also similar to those shown

in Figure 1 for the galaxy catalog.

We have computed the minimum  $\chi^2$  value of the 1-dimensional pairwise rms velocity of groups and particles from the comparison of the estimated (equation 2) and the actual values of  $\langle w^2 \rangle^{1/2}$ . By application of the first method described in section 3.1, we obtain  $\langle w^2 \rangle^{1/2} = 140 \pm 100 \text{ km s}^{-1}$  and  $\langle w^2 \rangle^{1/2} = 600 \pm 135 \text{ km s}^{-1}$  for groups and particles respectively, whereas the second method gives  $\langle w^2 \rangle^{1/2} = 430 \pm 85 \text{ km s}^{-1}$  and  $\langle w^2 \rangle^{1/2} = 530 \pm 70 \text{ km s}^{-1}$ . The results from the second method are in much better agreement with the actual values measured in the mock catalog than those from the first method (see table 3).

We have also calculated the projected 2-point correlation function for groups and particles from the mock catalogs. Using equation 8 we obtain estimates of correlation length,  $r_0 = 9.2 \pm 0.9 h^{-1} \text{ Mpc}$  for groups, and  $r_0 = 4.9 \pm 0.3 h^{-1} \text{ Mpc}$  for particles (see Figure 7). These values agree very well with the ones of the computational box ( $r_0 = 8.46 h^{-1} \text{ Mpc}$  and  $r_0 = 5.1 h^{-1} \text{ Mpc}$  for groups and particles, respectively), again indicating the efficiency of the methods adopted in deriving unbiased estimates of the parameter  $\beta$ . In effect, by means of equation 6 and with the derived parameters of the correlation function, we obtain  $\beta_{gr} < 0.35$  (one standard deviation) and  $\beta_{particles} = 0.61 \pm 0.22$ , which give a suitable agreement with the true values  $\beta_{gr} = 0.24$  and  $\beta_{particles} = 0.48$  respectively as can be appreciated in Figure 8.

We notice the differences between mock and real data (Figures 4 and 5 compared to Figures 7 and 8). These are mainly due to the different number of data points used, since we aimed to test the statistical procedures with catalogs with similar correlation and dynamical properties but with a larger number of points to improve accuracy to test for small systematic effects.

Taking into account the success of the different tests carried out, we conclude that the methods applied in section 3 give reliable estimates of the real-space clustering and mean rms pairwise velocity of groups and galaxies providing suitable estimates of the  $\beta$  parameter. The tests also indicate that the second method provides more stable and confident results of  $\langle w^2 \rangle^{1/2}$ .

## 5. CONCLUSIONS

Two-point correlation functions of groups and galaxies were computed from the UZC. The correlation function  $\xi(\sigma, \pi)$  in the components parallel and perpendicular to the line of sight, allow us to characterize the pairwise peculiar velocities. The distortions in  $\xi(\sigma, \pi)$  are considered by the convolution of the real-space correlation function  $\xi(r)$  with the pairwise velocity distribution  $f(w)$  (eq. 2). We have adopted an exponential model according to eq. 3 and we have used two methods to infer  $\langle w^2 \rangle^{1/2}$ . The first method compares the model  $\xi(\sigma, \pi)$  to the data in fixed  $\sigma$  bins, while the second method compares contours of constant predicted and observed correlation function. We use a minimum  $\chi^2$  method to obtain the best fitting values of  $\langle w^2 \rangle^{1/2}$ . More stable results come from the comparison of correlation level contours, where we obtain  $\langle w^2 \rangle^{1/2} = 325 \pm 175 \text{ km s}^{-1}$  and  $\langle w^2 \rangle^{1/2} = 433 \pm 42 \text{ km s}^{-1}$  for groups and galaxies respectively.

We have estimated the real-space correlation function using a power-law fit  $\xi(r) = (r/r_0)^\gamma$  for groups and galaxies. The correlation length,  $r_0$ , is obtained from the projected correlation function  $W(\sigma)$ , using the values of  $\gamma$  derived from the correlation function in projected separations  $\omega(\sigma)$ . The best fitting values for the parameters are:  $\gamma = -1.6$  and  $r_0 = 8.6 \pm 3.1 h^{-1} \text{ Mpc}$  for groups, and  $\gamma = -1.8$  and  $r_0 = 5.2 \pm 0.15 h^{-1} \text{ Mpc}$  for galaxies. We have used these estimates of  $r_0$  to compute  $\langle w^2 \rangle^{1/2}$  for groups and galaxies. The results for groups remain unchanged at  $\langle w^2 \rangle_{gr}^{1/2} \sim 300 \text{ km s}^{-1}$ . For galaxies, the comparison at constant  $\sigma$  bins gives values of  $\langle w^2 \rangle_{gx}^{1/2}$  as low as  $200 \text{ km s}^{-1}$ ; on the other hand, the comparison at constant  $\xi$  levels has a better agreement with the results shown in section 4,  $\langle w^2 \rangle^{1/2} \sim 500 \text{ km s}^{-1}$ , indicating the reliability of this procedure.

The results show a good agreement well to those obtained in other optical surveys (e.g., Loveday et al. (1992), Loveday et al. (1995), Lin et al. (1996), and Ratcliffe et al. (1998b)). For instance, our value of  $\langle w^2 \rangle_{gx}^{1/2} = 433 \pm 42 \text{ km s}^{-1}$  is entirely consistent with  $\langle w^2 \rangle_{gx}^{1/2} = 416 \pm 36 \text{ km s}^{-1}$ , obtained for the Durham-UKST Galaxy Redshift Survey by Ratcliffe et al. (1998b). Our determination of the real-space correlation length  $r_0 = 5.20 \pm 0.15 h^{-1} \text{ Mpc}$  is also comparable to that obtained in this survey  $r_0 = 5.1 \pm 0.3 h^{-1} \text{ Mpc}$  (Ratcliffe et al. (1998a)), although  $\xi(r)$  is

steeper in UZC ( $\gamma = -1.8$ ) compared to  $\gamma \simeq -1.6$  in the Durham-UKST redshift survey.

We have also estimated the parameter  $\beta = \Omega^{0.6}/b$  for groups and galaxies using the linear approximation relating real and redshift-space correlation functions. Consistent with previous works for other optical samples (e.g., Ratcliffe et al. (1998b), Loveday et al. (1996)) we find  $\beta_{gx} = 0.52 \pm 0.09$ . Results for IRAS samples (Fisher et al. 1994, Tadros et al. 1999) are similar to those derived for optical samples in spite of their different bias parameters. As suggested by Fisher et al. there may be a scale dependent galaxy biasing, although it should also be considered the possibility that different methods sensitive to a variety of factors may provide different results for a given sample.

For groups the results are noisy and do not allow a reliable estimate of the  $\beta$  parameter.

The reliability of our results has been tested using mock catalogs extracted from N-body simulations and the identification of three dimensional groups in these catalogs. The correlation function of groups and particles in  $\sigma$  and  $\pi$  coordinates show a similar behavior than the one derived from the observations.

The estimated and real values of the dimensional pairwise rms velocity of groups and particles in the simulations are comparable showing that our procedure is capable of deriving reasonable estimates of  $\langle w^2 \rangle_{gx}^{1/2}$  and  $\langle w^2 \rangle_{gr}^{1/2}$ . Also, the best fitting parameters  $r_0$  and  $\gamma$  for the group and particle correlation function are in excellent agreement with the true values in the three di-

mensional box indicating that our methods provide good estimates of the parameter  $\beta$ .

Given this fair agreement between derived and true values we conclude that the small angle approximation adopted in the analysis does not lead to systematic effects. A similar argument holds for the derivation of the  $\beta$  parameter using Kaiser (1986) linear formula which gives a very good agreement with the actual value in the simulation, supporting the reliability of the parameter  $\beta$  derived from UZC galaxies.

Spurious large anisotropies along the line of sight obtained for Abell clusters (e.g., Sutherland (1991)) are significantly reduced in the analysis of the APM cluster survey (Dalton (1992)). These large anisotropies would arise by inhomogeneities in the detection of clusters in two dimensions and are entirely absent in GUZC sample which shows the compression due to the infall onto larger structures. The main reason why these anisotropies are not present in GUZC is the that the groups are identified in an homogeneous catalog with angular positions and redshifts. The low value derived for the one-dimensional pairwise rms velocity of groups  $\langle w^2 \rangle^{1/2} = 325 \pm 175 \text{ km s}^{-1}$  is indicative of a smoothly varying peculiar velocity field from galaxies to systems of galaxies, as expected in a hierarchical scenario of structure formation.

We thank the Referee for helpful comments and suggestions which greatly improved the previous version of this paper. This work was partially supported by CONICET, SeCyT UNC and Fundación Antorchas, Argentina. MAGM acknowledges CNPq grant 301366/86-1.

## REFERENCES

- Abadi, M.G., Lambas, D.G. & Muriel, H. 1998, ApJ 507, 526.  
 Bean, A.J., Efstathiou, G., Ellis, R.S., Peterson, B.A., & Shanks, T. 1983, MNRAS 205, 605.  
 Croft, R.A.C., Dalton, G.B., Efstathiou, G., Sutherland, W.J. & Maddox, S.J. 1997, MNRAS 291, 305.  
 Dale, D.A.; Giovanelli, R., Haynes, M.P., Campusano, L.E., & Hardy, E. 1999, AJ 118, 1468.  
 Dalton, G.B., 1992, Doctoral Thesis, University of Oxford.  
 Davis, M., & Peebles, P.J.E., 1983, ApJ, 267, 465.  
 Falco, E.E., Kurtz, M.J., Geller, M.J., Huchra, J.P., Peters, J., Berlind, P., Mink, D.G., Tokarz, S.P., & Elwell, B. 1999, PASP 111, 438.  
 Huchra, J.P., & Geller, M.J. 1982, ApJ 257, 423.  
 Kaiser, N. 1987, MNRAS 227, 1.  
 Lin, H., Kirshner, R.P., Shectman, S.A., Landy, S.D., Oemler, A., Tucker, D.L., Schechter, P.L., 1996, ApJ, 471, 617L.  
 Loveday, J., Efstathiou, G., Peterson, B.A., & Maddox, S.J. 1992, ApJ 400, 43L.  
 Loveday, J., Maddox, S.J., Efstathiou, G., & Peterson, B.A. 1995, ApJ 442, 457.  
 Loveday, J., Efstathiou, G., Maddox, S.J., & Peterson, B.A. 1996, ApJ 468, 1.  
 Maia, M.A.G., da Costa, L.N., & Latham, D.W. 1989, ApJS 69, 809.  
 Merchán, M.E., Maia, M.A.G. & Lambas, D. 2000, ApJ, 544, 2.  
 Peacock, J.A. 1997, MNRAS, 284, 885.  
 Ramella, M., Pisani, A., & Geller, M.J., 1997, AJ 113, 483.  
 Ratcliffe, A., Shanks, T., Parker, Q.A., & Fong, R. 1998, MNRAS 296, 173.  
 Ratcliffe, A., Shanks, T., Parker, Q.A., & Fong, R. 1998, MNRAS 296, 191.  
 Sutherland, W.J. 1988, MNRAS 234, 159.  
 Sutherland, W.J., & Efstathiou G., 1991, MNRAS 248, 159.

- Tadros, H., Ballinger, W.E., Taylor, A.N., Heavens, A.F., Efstathiou, G., Saunders, W., Frenk, C.S., Keeble, O., McMahon, R., Maddox, S.J., Oliver, S., Rowan-Robinson, M., Sutherland, W.J., White, S.D.M., 1999, MNRAS, 305, 527.
- Valotto, C.A., Moore, B. & Lambas, D.G. 2000, ApJ, submitted.
- van Haarlem, M.P., Frenk, C.S., & White, S.D. 1997, MNRAS 287, 81.

TABLE 1  
PAIRWISE VELOCITY DISPERSION WITH FIRST METHOD: GALAXIES AND PARTICLES

$\sigma[h^{-1}Mpc]$	$\langle w^2 \rangle_{gx}^{1/2} [km/s]$	$\langle w^2 \rangle_{mock\ gx}^{1/2} [km/s]^{(1)}$
0.5	$430 \pm 59$	$600 \pm 122$
1.5	$560 \pm 106$	$500 \pm 117$
2.5	$650 \pm 112$	$890 \pm 164$
3.5	$810 \pm 140$	$560 \pm 121$
4.5		$640 \pm 178$
5.5		$500 \pm 194$

<sup>(1)</sup> Actual value  $\langle w^2 \rangle_{mock\ gx}^{1/2} = 520\ km/s$ .

TABLE 2  
PAIRWISE VELOCITY DISPERSION WITH FIRST METHOD: UZC AND MOCK GROUPS

$\sigma[h^{-1}Mpc]$	$\langle w^2 \rangle_{gr}^{1/2} [km/s]$	$\langle w^2 \rangle_{mock\ gr}^{1/2} [km/s]^{(1)}$
1.5	$460 \pm 198$	$410 \pm 101$
4.5	$360 \pm 189$	$50 \pm 89$
7.5	$360 \pm 170$	$10 \pm 153$
10.5		$30 \pm 105$

<sup>(1)</sup> actual value  $\langle w^2 \rangle_{mock\ gr}^{1/2} = 400\ km/s$

TABLE 3  
PAIRWISE VELOCITY DISPERSION WITH SECOND METHOD

$\xi$	$\langle w^2 \rangle_{gx}^{1/2} [km/s]$	$\langle w^2 \rangle_{mock\ gx}^{1/2} [km/s]^{(1)}$	$\langle w^2 \rangle_{gr}^{1/2} [km/s]$	$\langle w^2 \rangle_{mock\ gr}^{1/2} [km/s]^{(2)}$
0.6	$430 \pm 43$	$500 \pm 82$	$340 \pm 156$	$400 \pm 185$
0.8	$430 \pm 28$	$550 \pm 71$	$250 \pm 156$	$420 \pm 130$
1.0	$480 \pm 39$	$470 \pm 92$	$240 \pm 140$	$410 \pm 95$
1.2	$540 \pm 37$	$530 \pm 61$	$240 \pm 88$	$420 \pm 63$
1.4	$430 \pm 34$	$560 \pm 50$	$240 \pm 85$	$450 \pm 64$

<sup>(1)</sup> actual value  $\langle w^2 \rangle_{mock\ gx}^{1/2} = 520\ km/s$ .

<sup>(2)</sup> actual value  $\langle w^2 \rangle_{mock\ gr}^{1/2} = 400\ km/s$

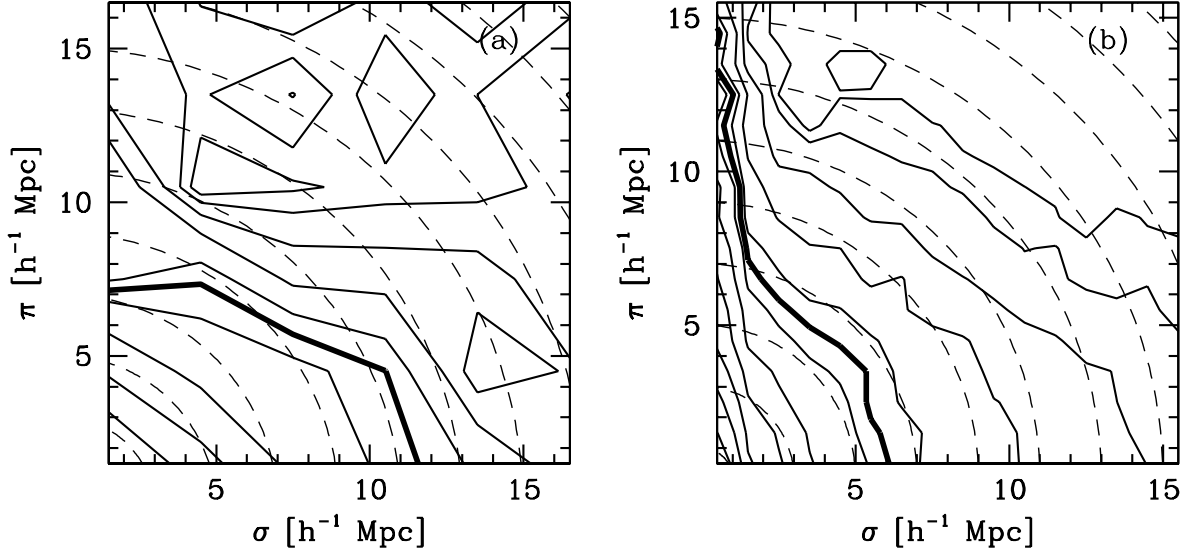


FIG. 1.— Contour map of the correlation function  $\xi(\sigma, \pi)$  estimated from the UZC as a function of separations parallel ( $\pi$ ) and perpendicular ( $\sigma$ ) to the line of sight. The contours correspond to fixed steps in  $\log(\xi)$  from  $-0.8$  to  $1$ . The transition to the linear regime,  $\xi(\sigma, \pi) = 1$  level, is shown as a thick contour. For comparison, dashed lines correspond to undistorted level contours. panel a) is for groups, while panel b) is for galaxies.

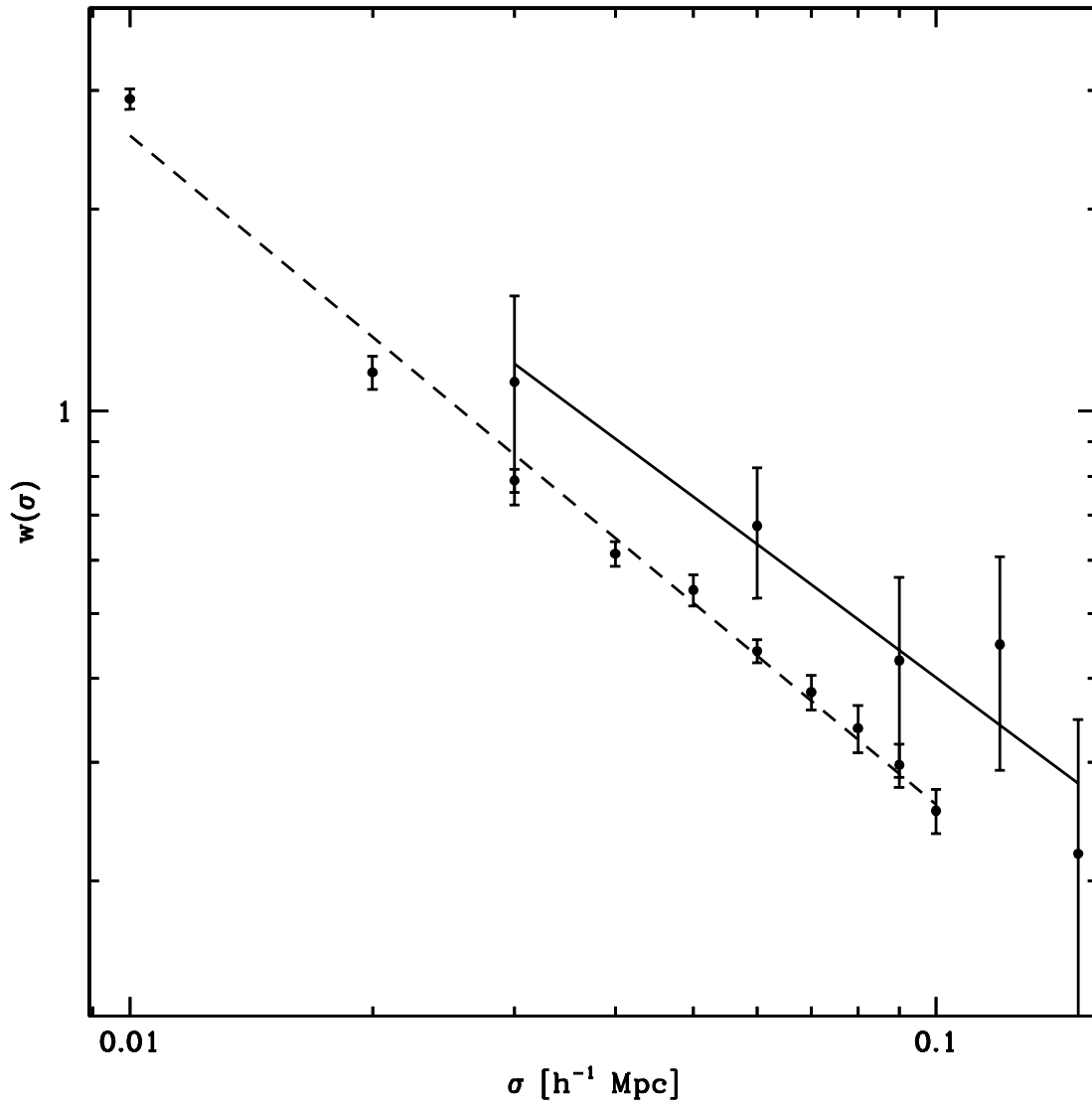


FIG. 2.— Projected two-point correlation functions  $w(\sigma)$  of UZC galaxies and groups. Solid and dashed lines correspond to the best power law fits  $A\sigma^\gamma$ , with  $\gamma = -0.89$  for groups and  $\gamma = -1.0$  for galaxies respectively.

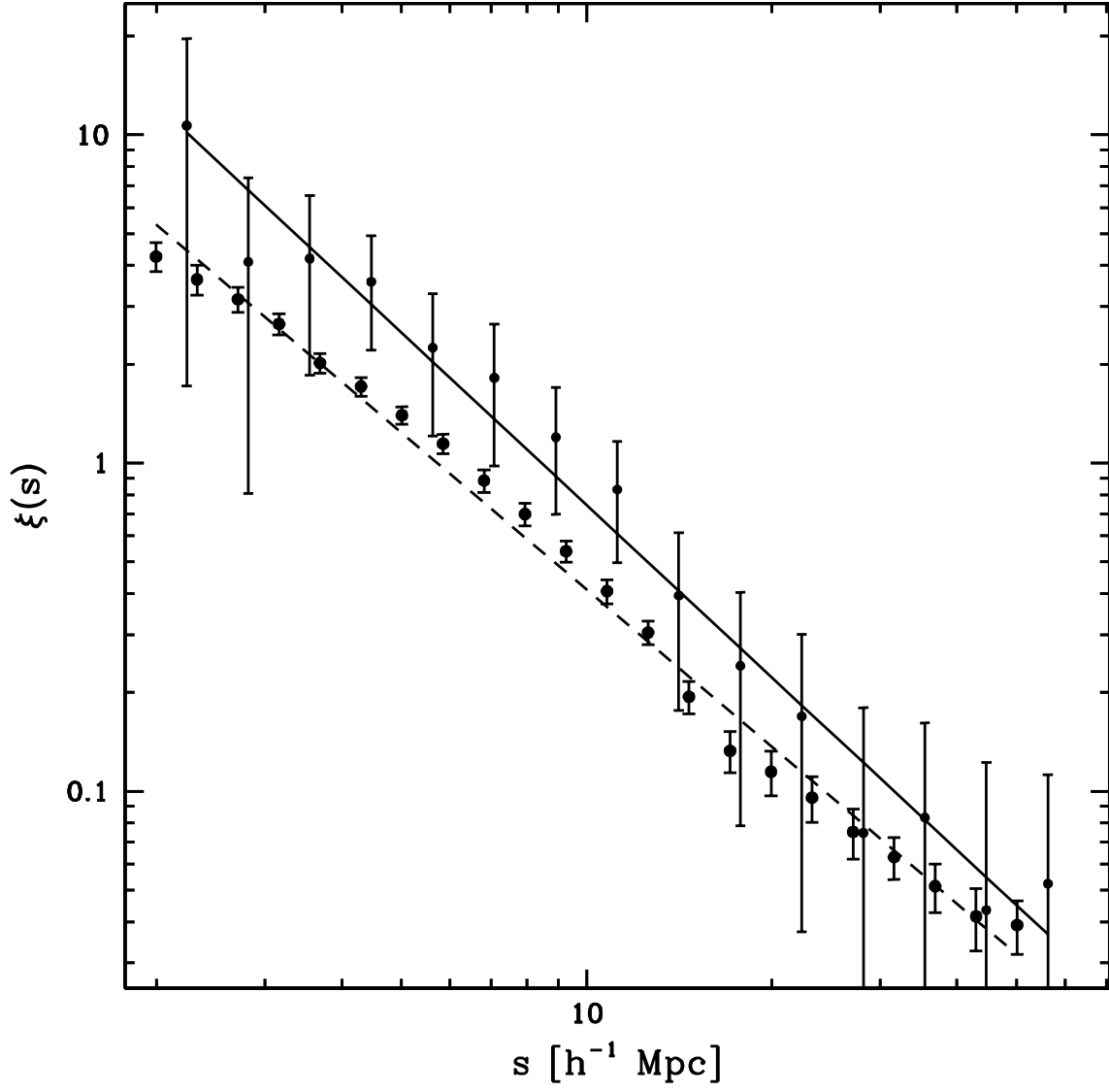


FIG. 3.— Redshift-space autocorrelation function ( $\xi(r)$ ) for galaxies and groups. Error bars correspond to Poisson estimates of uncertainties. Solid and dashed lines show power law fits  $(r/r_0)^\gamma$  with  $r_0 = 9.8 \, h^{-1} \text{ Mpc}$ ,  $\gamma = -1.59$  (groups) and  $r_0 = 6.4 \, h^{-1} \text{ Mpc}$ ,  $\gamma = -1.45$  (galaxies) respectively.

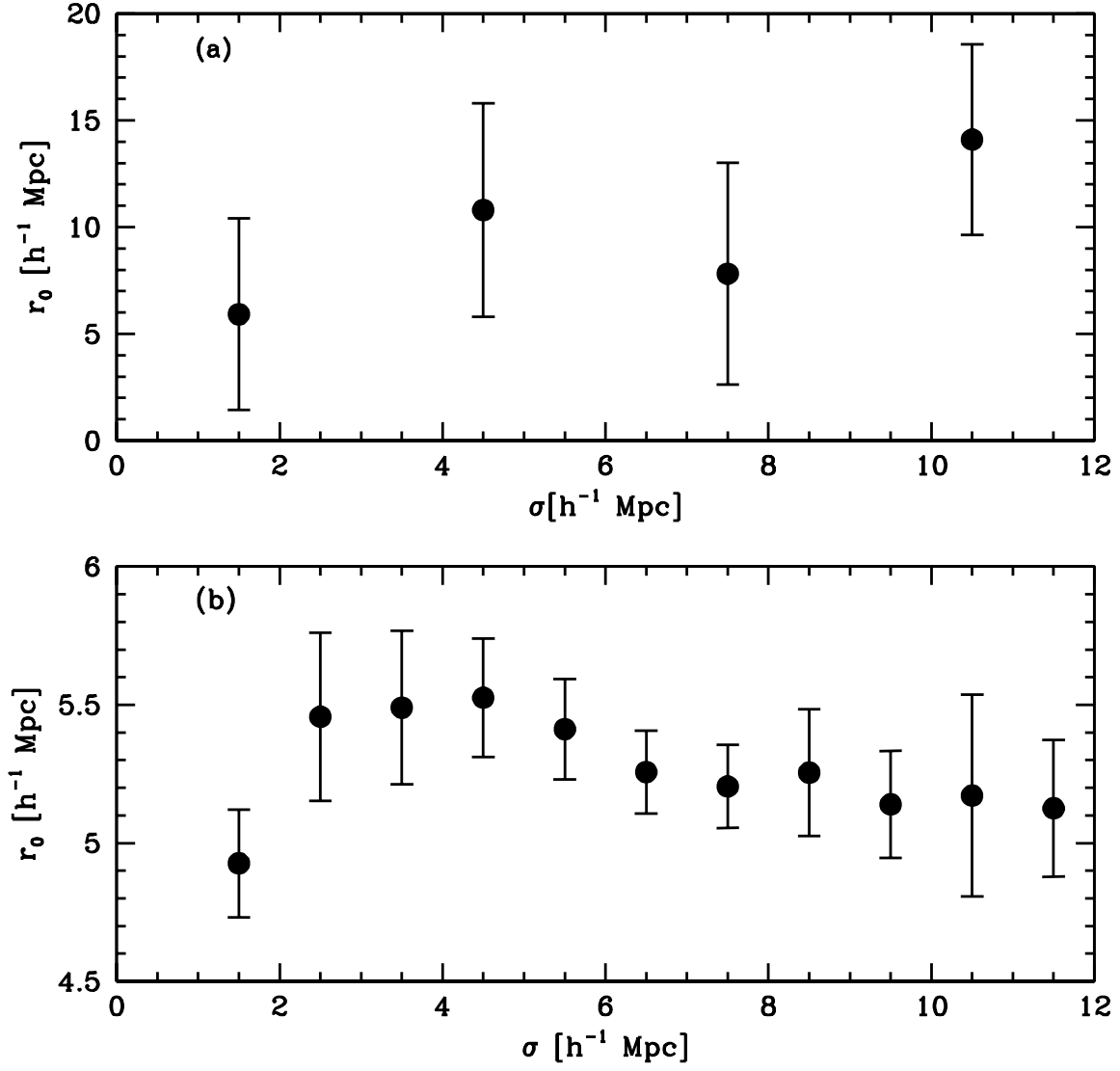


FIG. 4.— Estimates of real-space correlation length  $r_0$  derived from the projected correlation function  $W(\sigma)$  eq. 8. Errorbars correspond to direct estimates from bootstrap resamplings. a) UZC groups, b) UZC galaxies.

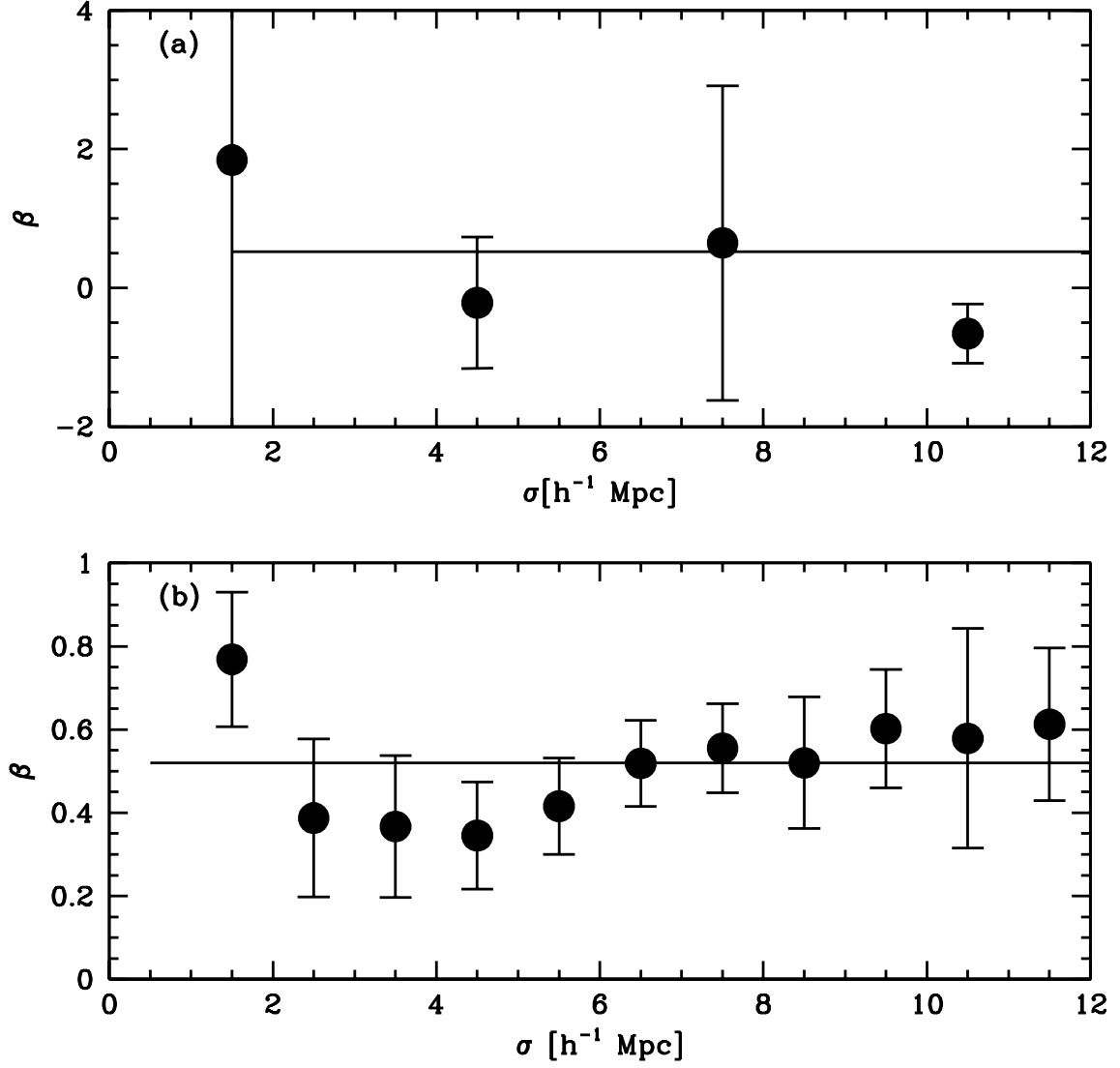


FIG. 5.— Estimates of  $\beta$  for UZC groups derived from equation 6. Errorbars correspond to propagation of errors in eq. 6 from errors in  $r_0$  quoted in figure 6. The solid line corresponds to the best  $\chi^2$  estimate of  $\beta$  from galaxies. a) UZC groups, b) UZC galaxies.

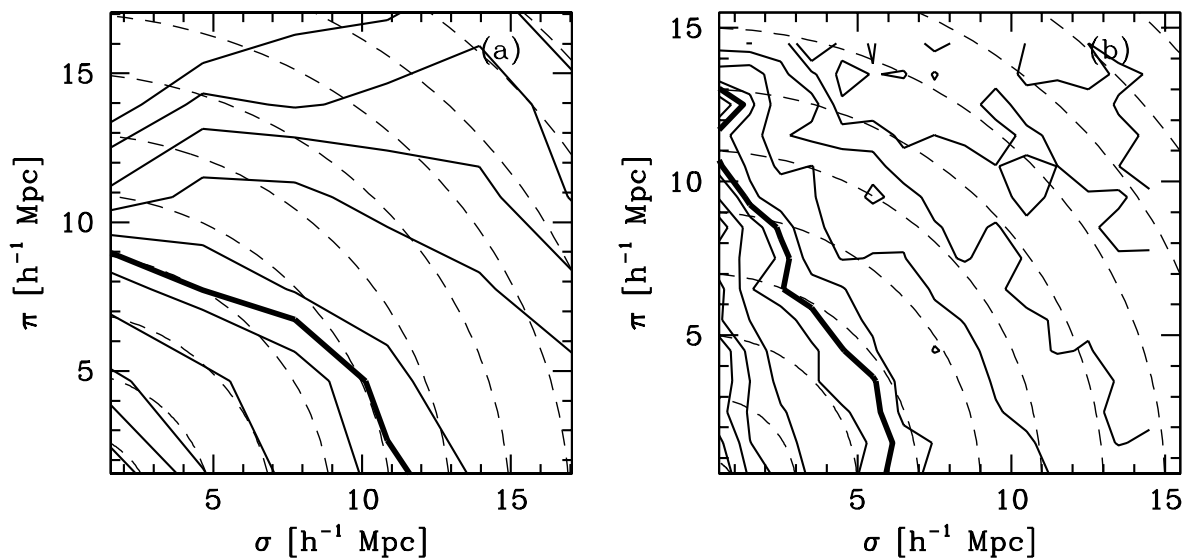


FIG. 6.— Contour map of the correlation function  $\xi(\sigma, \pi)$  estimated from the mock catalogs as a function of separations parallel ( $\pi$ ) and perpendicular ( $\sigma$ ) to the line of sight. The contours correspond to fixed steps in  $\log(\xi)$  from  $-0.8$  to  $1$ . The transition to the linear regime, at  $\xi(\sigma, \pi) = 1$  level, is shown as a thick contour. For comparison, dashed lines correspond to undistorted level contours. Panel a) is for mock groups, while panel b) is for mock galaxies.

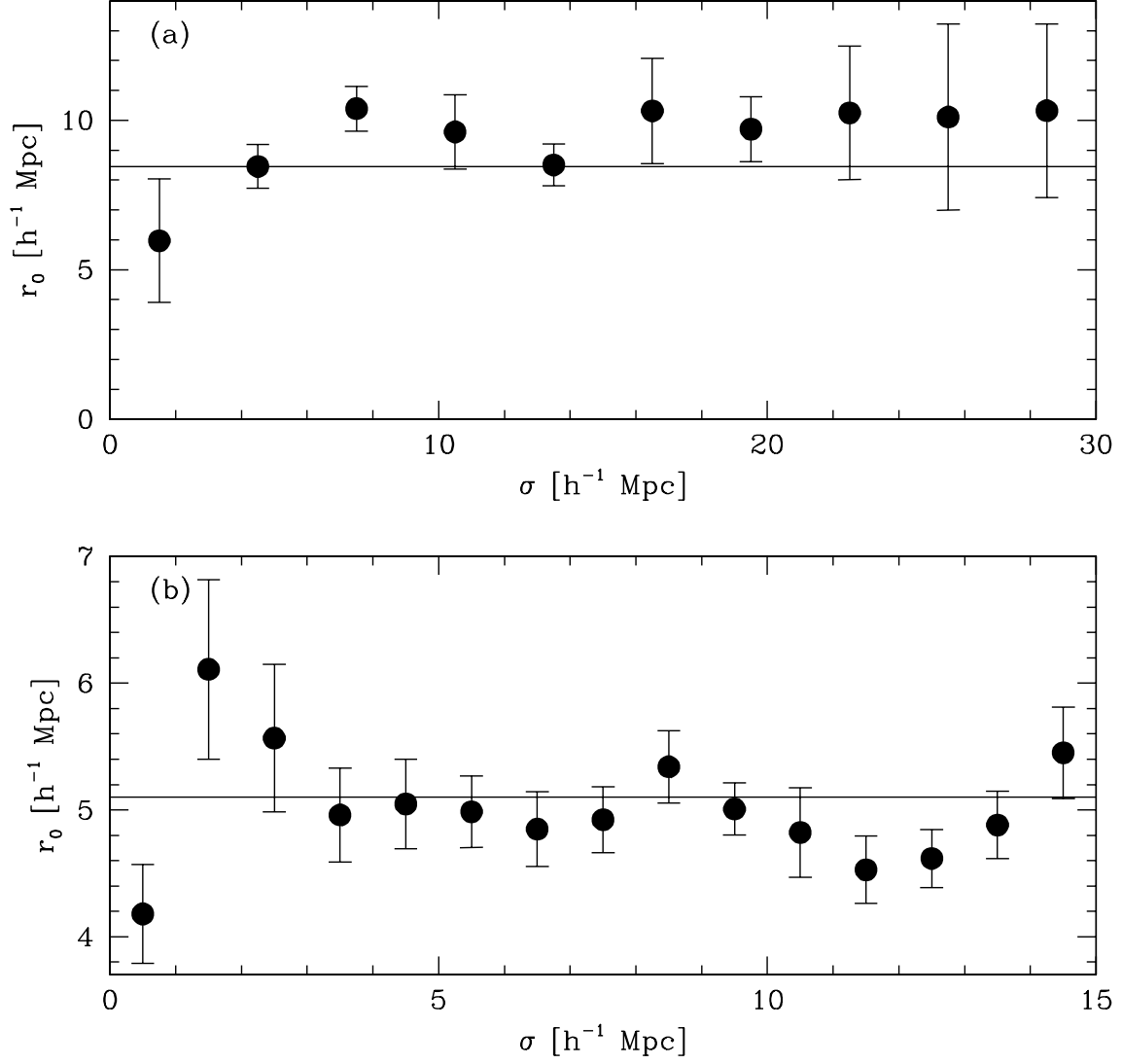


FIG. 7.— Estimates of real-space correlation length  $r_0$  derived from the projected correlation function  $W(\sigma)$  eq. 8. a) mock groups, b) mock galaxies. Errorbars correspond to direct estimates from bootstrap resamplings. The solid line corresponds to the true values of  $r_0$  of galaxies and groups in the numerical simulation.

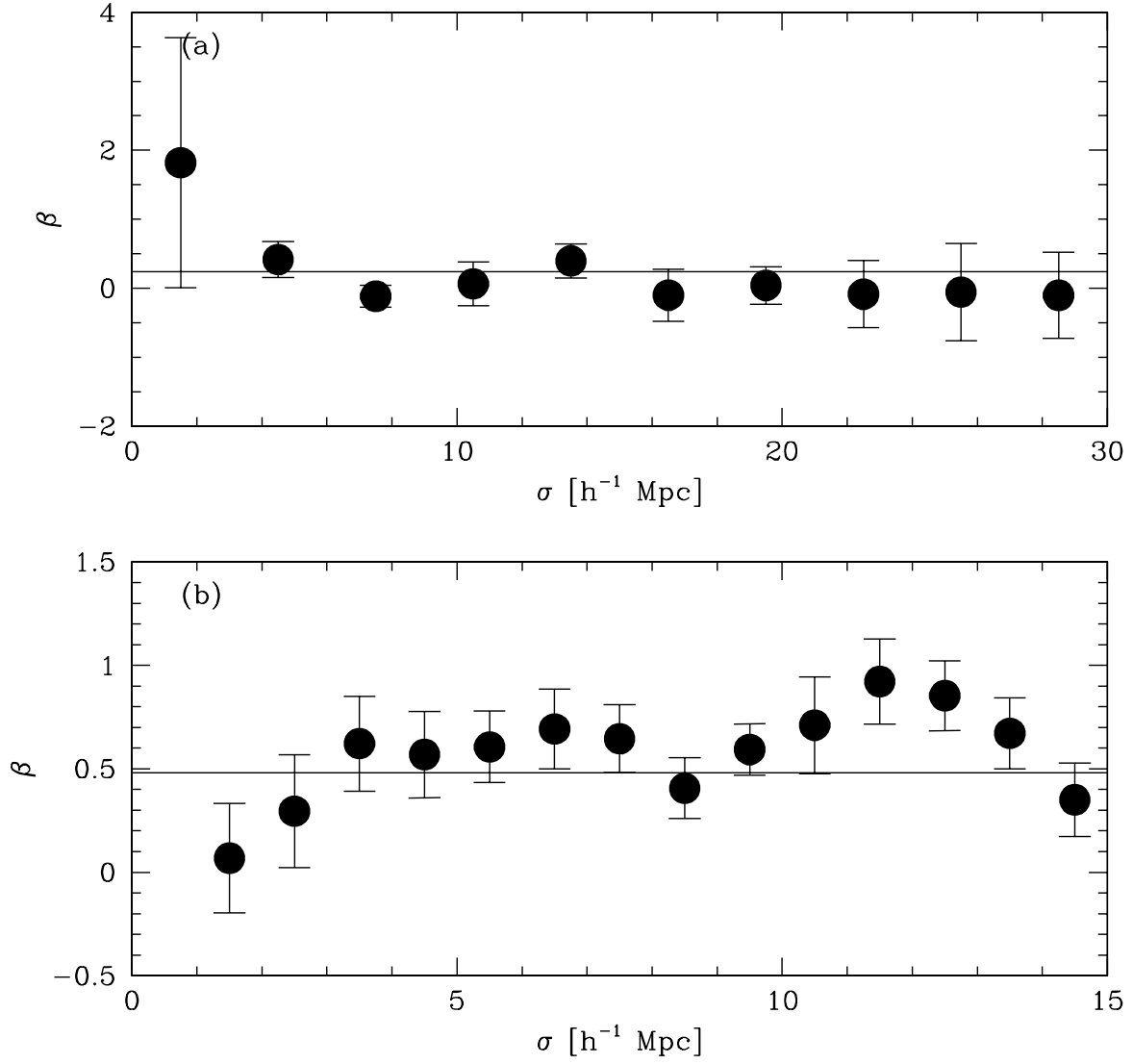


FIG. 8.— Estimates of  $\beta$  for mock groups derived from equation 6. a) mock groups, b) mock galaxies. Errorbars correspond to propagation of errors in eq. 6 from errors in  $r_0$  quoted in figure 6. The solid line corresponds to the true values of  $\beta$  of galaxies and groups in the numerical simulation.